Supporting Information for:

INORGANIC PHOTOTROPISM IN ELECTRODEPOSITION OF SE-TE

MADELINE C. MEIER[†], WEN-HUI CHENG[‡], HARRY A. ATWATER[‡,§], NATHAN S. LEWIS[‡,§,ǁ*]

AND AZHAR I. CARIM[†]

[†]Division of Chemistry and Chemical Engineering

[‡]Division of Engineering and Applied Sciences

[§]Kavli Nanoscience Institute

[ǁ]Beckman Institute

California Institute of Technology

Pasadena, CA 91125

*Corresponding Author: nslewis@caltech.edu

S1. Contents

This document contains a description of the experimental and modeling/simulation methods utilized in this work (Sections S2 and S3), additional scanning-electron micrographs (Section S4), analyses of the elemental composition and structure of the photoelectrodeposits (Section S5), voltammetric data (Section S6), and a list of associated references (Section S7).

S2. Experimental Methods

Materials and Chemicals Buffered HF improved etchant (Transene), poly(methyl methacrylate) (PMMA, Microchem), methyl isobutyl ketone (99.9 %, VWR), isopropanol (99.5 %, VWR), Ti (99.995 %, Kurt J. Lesker), Au (99.999 %, Materion), In (99.999 %, Alfa Aesar), Ga (99.999 %, Alfa Aesar), H_2SO_4 (ACS Reagent, J. T. Baker), SeO_2 (99.4 %, Alfa Aesar), and TeO_2 (99+ %, Sigma-Aldrich) were used as received. H_2O with a resistivity ≥ 18.2 MΩ cm (Barnstead Nanopure System) was used throughout. Au-coated n^+-Si(100) (< 0.005 Ω cm, As-doped, 525 ± 25 μm thick, single-side polished, Addison Engineering) was used as a substrate for deposition. Flash-Dry Ag Paint (SPI Supplies), EP21ARHTND Epoxy (MasterBond) and nitrocellulose-based nail polish were used to assemble the working electrodes.

Substrate Preparation n^+-Si wafers were rinsed with acetone and isopropanol. A bilayer resist for electron-beam lithography composed of poly(methyl methacrylate) (PMMA) was then applied by spin-coating. First, a base layer of 495 PMMA A4 was applied at 4000 rpm for 1.0 min and baked at 180 °C for 3.0 min. Second, an overlayer of 950 PMMA A4 was applied at 4000 rpm for 1.0 min and baked at 180 °C for 3.0 min. Next, a VISTEC EBPG 5000+ electron-beam pattern generator was used to pattern the resist into a square lattice of 150 nm diameter circles on an 8 μm pitch. Pattern generation was effected using a 100 kV accelerating voltage, 300 μm aperture, 5 nA current, and a dose of 1000 μC cm^{-2}. After electron-beam pattern generation, the substrates were immersed in mixture of methyl isobutyl ketone : isopropanol in a 1 : 3 volume ratio for 1.0 min at room temperature, to develop the pattern and produce arrays of holes. Next, the substrates were etched with buffered HF for 1.0 min, rinsed with H_2O, dried under a stream of N_2(g), and then immediately transferred to a CHA Mark 40 electron-beam metal evaporator with a base pressure of 10^{-6} torr. A 5 nm thick Ti adhesion layer was first

deposited at a rate of 0.05 nm s^{-1} and then a 50 nm thick Au layer was deposited at a rate of 0.10 nm s^{-1}. The substrates were removed from the evaporator and immersed in acetone to remove the remaining resist, yielding a Si substrate patterned with Au/Ti circles. The patterned substrates were then cut into square 0.50 cm by 0.50 cm pieces using a Dynatex GST-150 scriber-breaker system, and were used as substrates for photoelectrochemical deposition of Se-Te.

Electrode Preparation Electrode assemblies were prepared by applying epoxy to the flat sides of each of two Al half-round bars (0.25 in diameter). The two bars were then joined together, with an ~ 10 mm offset in the axial dimension to form a cylinder with two half-round ends. Polytetrafluoroethylene heat-shrink tubing was used to insulate the cylindrical section and epoxy was used to insulate the rounded side of one of the half-round ends. A eutectic mixture of Ga and In was scratched with a carbide-tipped scribe into the unpolished back surfaces of the Au-topped Si sections. Ag paint was then applied to the eutectic and the Au-topped Si section was affixed to the flat surface of the epoxied half-round end. Nail polish was used to insulate the remaining uncovered area on the flat surface that surrounded the Au-topped Si section. Figure S1 presents a schematic of an electrode assembly with an attached Au-topped Si section. Immediately before deposition, the surface of each electrode was briefly cleaned using a stream of $N_2(g)$.

Figure S1. Schematic of an electrode assembly with an attached Au-topped Si section.

Electrode Illumination Photoelectrochemical depositions were performed using narrow-band light-emitting diode (LED) sources (Thorlabs) having intensity-weighted average wavelength, λ_{avg}, values and spectral bandwidths (FWHM) of 528 nm and 32 nm (SOLIS-525C), 727 nm and 37 nm (M730L4), and 843 nm and 30 nm (M850L3), respectively. The output of each diode source was collected and collimated with an aspheric condenser lens (Ø50.8 mm, f = 32 mm). A 1500 grit ground-glass (UV Fused Silica) diffuser was placed immediately in front of the photoelectrochemical cell to ensure spatial homogeneity of the illumination. The light intensity incident on the electrode was measured by placing a calibrated Si photodiode (Thorlabs FDS100), instead of an electrode assembly, in the photoelectrochemical cell with electrolyte, and the steady-state current response of the Si photodiode was measured. Depositions utilizing illumination at normal incidence and the diode with λ_{avg} = 528 nm were performed with a light intensity of 20 mW cm^{-2}. Depositions under illumination at normal incidence utilizing the diodes with λ_{avg} = 727 nm and 843 nm were performed with a light intensities of 40 mW cm^{-2}, and 50 mW cm^{-2}, respectively. To compensate for the decrease in the optical extinction coefficient of the

Se-Te alloy with increasing wavelength from the visible to the near-infrared regime, photoelectrochemical growth with near-infrared illumination inputs was performed with greater optical intensities than were utilized for the visible illumination input. The higher illumination intensities utilized in conjunction with λ_{avg} = 727 nm or λ_{avg} = 843 nm relative to λ_{avg} = 528 nm were selected to effect the same rate of photoelectrochemical growth for each wavelength input. For depositions using illumination incident on the electrode at an angle α away from the surface normal, the intensities were increased by a factor of $\cos^{-1}(\alpha)$ relative to the intensities used at normal incidence.

Photoelectrochemical Deposition Photoelectrochemical deposition was performed using a Bio-Logic SP-200 potentiostat. Deposition was performed in a glass cell with a pyrex window. A three-electrode, two-compartment cell was used with an Ir wire counter electrode (99.999 %, Sigma-Aldrich) isolated behind a porous glass frit, and a Ag/AgCl reference electrode (3 M KCl, Bioanalytical Systems). In this configuration, current was sourced only between the working electrode and the counter electrode, preventing any deleterious concentration changes in the Ag/AgCl reference electrode. Films were deposited from an aqueous solution of 0.0200 M SeO_2, 0.0100 M TeO_2, and 2.00 M H_2SO_4. Deposition was effected by biasing the Au-coated electrode, illuminated as described above (*Electrode Illumination*), potentiostatically at -0.15 V vs. Ag/AgCl for 3.00 min at room temperature (unless otherwise noted). After deposition, the electrode was immediately removed from the cell, rinsed with H_2O, and then dried under a stream of N_2(g). The patterned substrate with the top-facing Se-Te deposit was mechanically separated from the rest of the electrode assembly. The nitrocellulose-based insulation and the majority of the Ag paint and In-Ga eutectic were then removed mechanically.

Microscopy Scanning-electron micrographs (SEMs) were obtained with a FEI Nova NanoSEM 450 with a working distance of 5 mm and an in-lens secondary electron detector. Top-down micrographs were acquired using an accelerating voltage of 5.00 kV and cross-sectional micrographs were acquired using an accelerating voltage of 15.00 kV. All micrographs were acquired with a resolution of 344 pixels μm^{-1}.

Energy-dispersive X-Ray Spectroscopy Energy dispersive X-ray (EDX) spectroscopy was performed in the SEM using an accelerating voltage of 15.00 kV and a working distance of 5 mm. An Oxford Instruments X-Max silicon drift detector was utilized. Spectra were collected in the range of 0 to 10 keV and quantitative deposit compositions were derived from these spectra using the "INCA" software package (Oxford Instruments).

Raman Spectroscopy Raman spectra were collected with a Renishaw inVia Raman microprobe equipped with a Leica DM 2500 M microscope, a Leica N Plan 50x objective (numerical aperture = 0.75), an 1800 lines mm^{-1} grating, and a CCD detector configured in a 180° backscatter geometry. A 532 nm diode-pumped solid-state (DPSS) laser (Renishaw RL532C50) was used as the excitation source and a 10 μW radiant flux was incident on the surface of the sample. A λ/4 plate was used to circularly polarize the incident excitation. No polarizing collection optic was used.

S3. Modeling and Simulation Methods

Two-dimensional finite-difference time-domain (FDTD) simulations were used to model light absorption during morphological evolution of idealized photoelectrodeposit structures. Modeling was performed using the "FDTD Solutions" software package (Lumerical). Figure S2 presents a schematic diagram of the utilized simulation geometry. The simulations evaluated a hemispherical Se-Te semi-ellipsoid with diameter of 350 nm and height of 250 nm, grown about a columnar metal contact 150 nm in diameter consisting of 50 nm of Au atop 5 nm of Ti. The Ti was centered on a rectangular Si substrate with a width of 8.00 μm and a height of 0.50 μm. The area above the substrate surrounding the Se-Te deposit was considered to be filled with deposition electrolyte. Previously measured values of the complex index of refraction for Se-Te were utilized. A value of $n = 1.33$ was used for the refractive index of the electrolyte, regardless of wavelength.[1] The intensity-weighted average wavelength of the actual sources described in Section S2 were utilized. Two same-wavelength, coherent, completely out-of-phase sources, with the same propagation vector and orthogonal polarization vectors, were simulated to model unpolarized illumination. Bloch boundary conditions were utilized in the directions parallel to the substrate and perfectly matched layer boundary conditions were used in the perpendicular directions. Simulations were discretized using a uniform two-dimensional square mesh with a lattice constant of 2 nm.

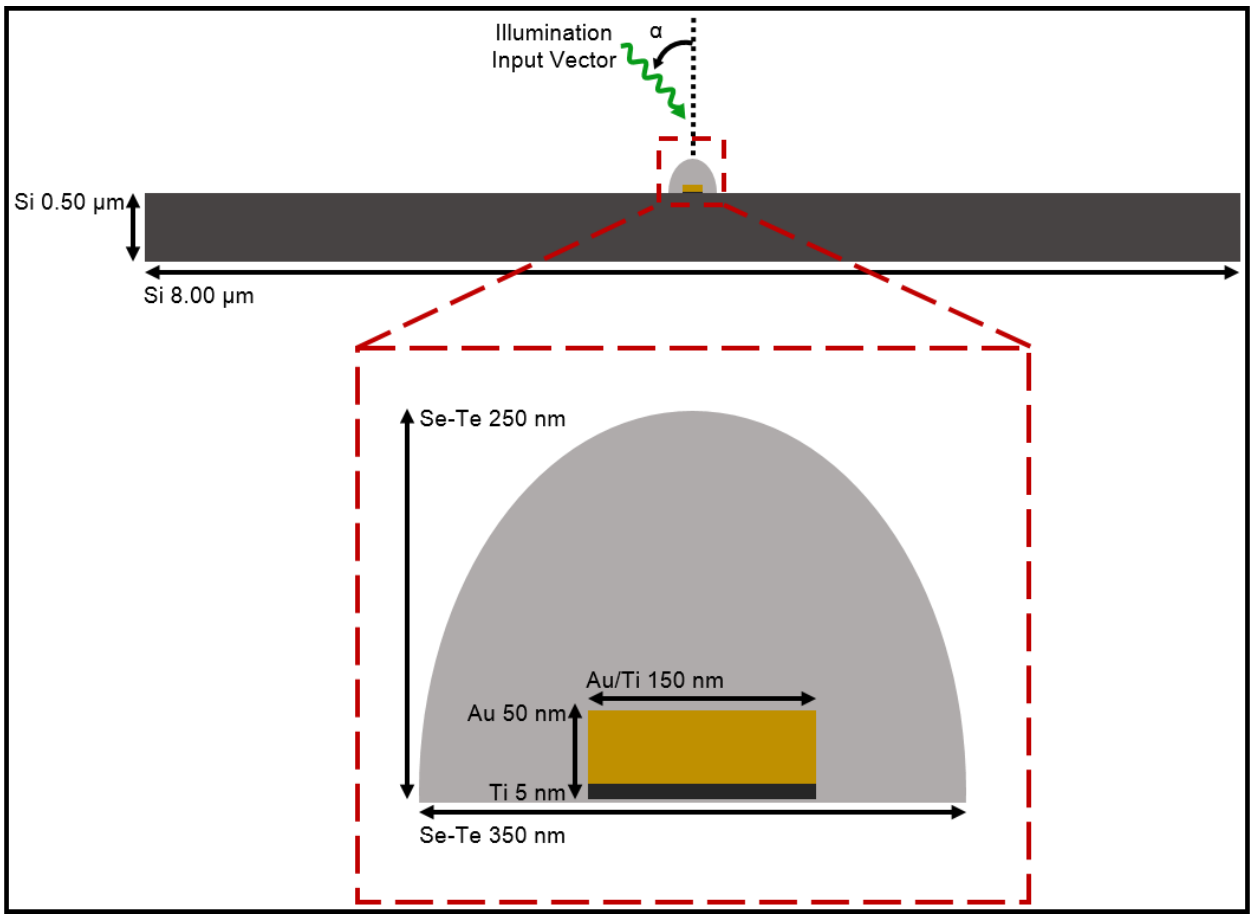

Figure S2. Schematic of the geometry utilized for light absorption modeling with idealized photoelectrodeposit structures.

S4. Additional Scanning-Electron Micrographs

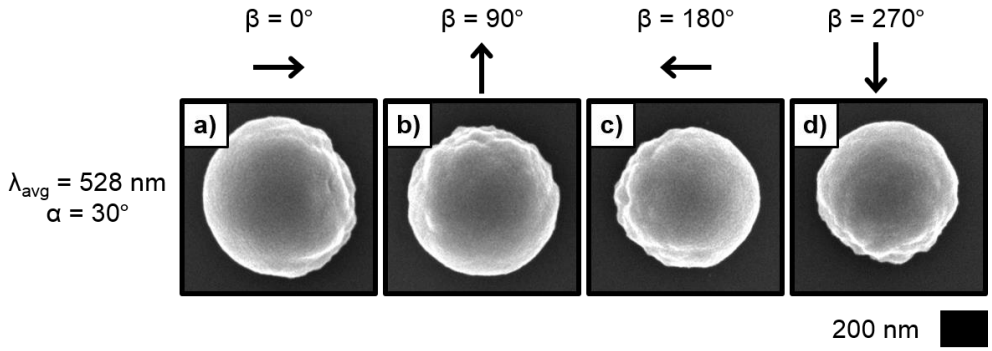

Figure S3. Top-down SEMs representative of photoelectrodeposits generated with λ_{avg} = 528 nm illumination incident at α = 30° from the substrate normal along the indicated in-plane direction β.

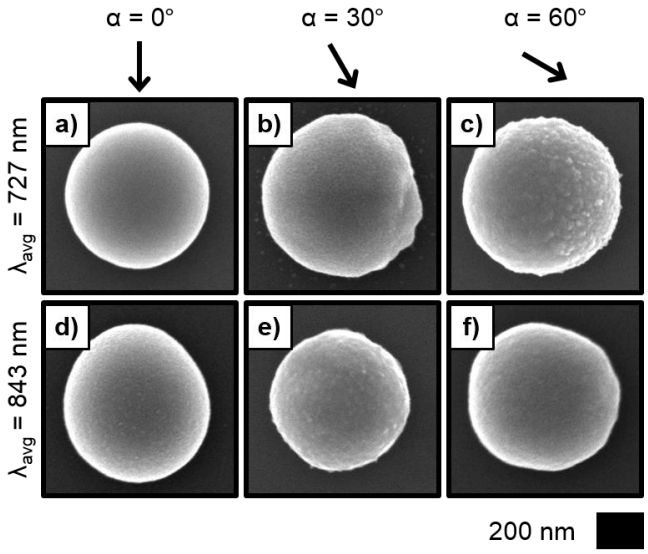

Figure S4. Top-down SEMs representative of photoelectrodeposits generated with the indicated λ_{avg} illumination incident at the indicated angle α from the substrate normal.

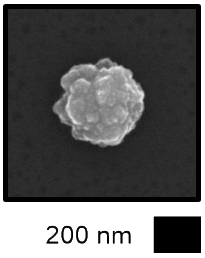

Figure S5. Top-down SEM representative of a deposit generated in the dark.

For the photoelectrodeposition described in this work, light-directed growth effects a smooth topology on the subwavelength scale (~ λ/10) as local rates of mass addition are dictated

by a similarly smooth light absorption profile. In contrast, dark growth, potentially dictated by electrochemical kinetics, exhibits roughness on this scale (Figure S5). Photoelectrodeposits generated with non-normally incident illumination ($\alpha > 0°$) may exhibit roughness on the far side away from the illumination incidence if the material absorption is sufficient to attenuate light propagation to the far side and the occurrence of light-directed growth there, relatively favoring dark growth.

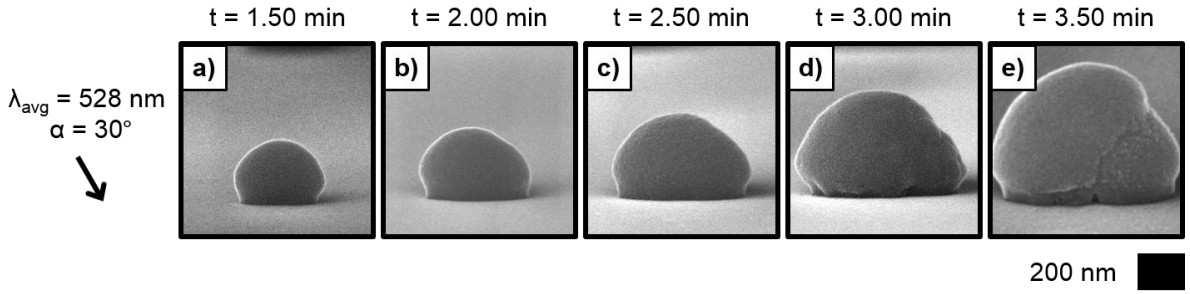

Figure S6. Cross-sectional SEMs representative of photoelectrodeposits generated with λ_{avg} = 528 nm illumination incident at $\alpha = 30°$ from the substrate normal and the indicated growth time.

S5. Compositional and Structural Analyses of Photoelectrodeposits

The elemental composition of photoelectrodeposits generated with a range of illumination inputs was analyzed using energy-dispersive X-ray (EDX) spectroscopy. All analyzed photoelectrodeposits were wholly composed of Se and Te, in statistically identical fractions (Table S1). These data indicated that the composition of the photoelectrodeposited material was independent of the illumination input for the investigated parameter space.

λ_{avg} / nm	α / °	Se Fraction / Atomic %
528	0	23 ± 6
528	30	24 ± 6
528	60	21 ± 6
727	0	23 ± 7
843	0	24 ± 6

Table S1. Composition of Se-Te alloy photoelectrodeposits generated with the indicated illumination inputs expressed in terms of Se atomic % (balance Te) as derived from EDX spectroscopic analysis.

Figure S7a presents representative Raman spectra of photoelectrodeposits generated using λ_{avg} = 528 nm illumination incident at an angle α = 0, 30 or 60° from the surface normal. Figure S7b presents Raman spectra of photoelectrodeposits generated using λ_{avg} = 528, 727 or 843 nm illumination incident at α = 0° from the surface normal. All of the spectra showed a mutually similar scattering profile, with two principal modes centered at 143 cm^{-1} and 174 cm^{-1}. The presence of these modes is consistent with a substitutional alloy of Se and Te in a trigonal structure common to each element in the pure phase. The relative intensity of the modes indicated the alloy was Te rich.[2] The observation of a consistent scattering profile for photoelectrodeposits generated with varying values of λ_{avg} and α suggests that the composition and structure of the photoelectrodeposited material was independent of the illumination inputs for the investigated parameter space.

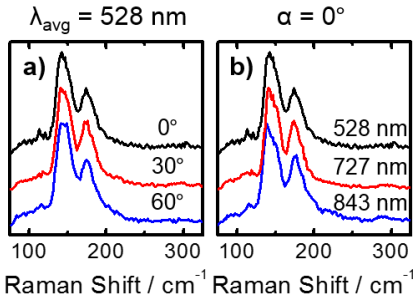

Figure S7. Representative Raman spectra of photoelectrodeposits generated with (a) λ_{avg} = 528 nm illumination incident at the labeled angle α from the substrate normal and (b) with the labeled λ_{avg} illumination incident at α = 0° from the substrate normal.

S6. Voltammetric Data

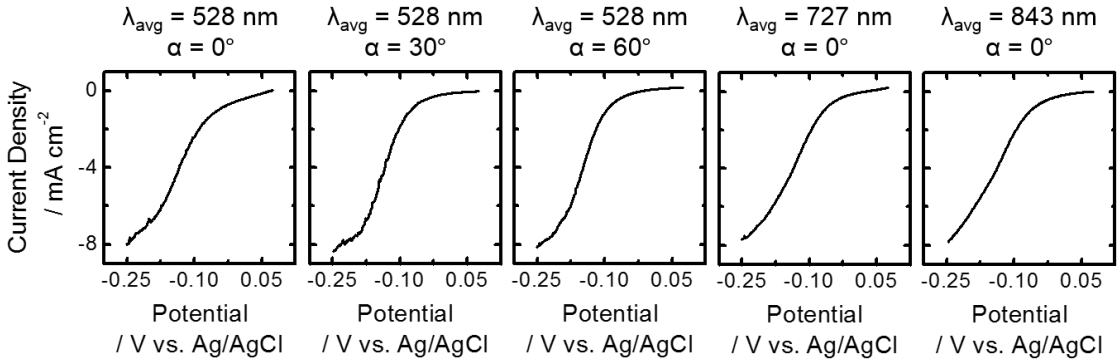

Figure S8. Representative voltammetric data (scan rate υ = 75 mV s^{-1}) for the photoelectrodeposition process using the indicated illumination inputs.

S7. References

(1) Hale, G. M.; Querry, M. R. *Appl. Opt.* **1973**, *12*, 555-563.
(2) Geick, R.; Steigmeier, E. F.; Auderset, H. *Phys. Status Solidi B* **1972**, *54*, 623-630.